Impact of anodic bonding on transmission loss in 23GHz pressure transducers

M.V. De Paolis[a,*], J. Philippe[a], A. Rumeau[a], A. Coustou[a], S. Charlot[a], H. Aubert[a], P. Pons[a]

[a] *LAAS-CNRS, University of Toulouse, CNRS, INP, INSA, Toulouse, France*

Abstract

This paper analyses the impact of anodic bonding technique on the transmission loss in 23GHz pressure transducers. The transducers consist of a thin high resistivity silicon membrane and a 23GHz planar resonator placed inside a cavity. Two types of transmission line are used here for designing the resonators: probe-fed coplanar lines and aperture-coupled microstrip ones. Transducers based on aperture-coupled microstrip resonators and manufactured from the anodic bonding process for assembling the silicon membrane to the glass substrate are the most promising low-loss solution. It is actually shown that, at the resonant frequency of the planar resonator, the measured transmission loss in a probe-fed coplanar transducer is about 4dB when using bonding with the photoresist as an intermediate layer, while it is only of 2.55dB when applying the anodic bonding assembling process. However, we report for the first time that very high and unexpected transmission loss (>30dB) occurs when using anodic bonding technique to manufacture the 23GHz aperture-coupled microstrip transducers.

1. Introduction

Anodic (or thermo-electric) bonding technology is intensively used for achieving airtight sealing, device integration, and vacuum packaging in micro-electro-mechanical systems (MEMS) and sensors [1]. This standard technique consists of applying at high temperature (400°C) a voltage of several hundred volts on two substrates in mechanical contact. The voltage enhances the occurrence of chemical bonds and as a result, this anodic bonding assembling technique may achieve the excellent bonding strength, and the good airtight sealing for cavity manufacturing [2].

For the first time, the impact on pressure transducers' performance of the anodic bonding process used for assembling the high resistivity silicon (HR-Si) wafer to the glass substrate is investigated in this paper. The pressure transducers based on two types of transmission lines and two bonding techniques are reported. The pressure transducers are composed of a 100µm thick HR-Si membrane, a cavity, and a planar resonator operating at 23GHz. The transducers' working principle is based on electromagnetic and mechanical transductions [3-5]. The pressure applied on the transducers leads to the membrane deformation and as a result, it changes the resonant frequency of the planar resonator.

Two planar technologies are used here for designing the transducers: the probe-fed coplanar line technology and the aperture-coupled microstrip line one. The airtight packaging cannot be easily achieved for probe-fed coplanar transducers, because it is difficult to feed the resonator from outside when it is enclosed into a cavity. Based on proximity electromagnetic coupling, the aperture-coupled technique allows feeding more easily resonators in their cavity than the previous approach. Moreover, it facilitates the full integration of the resonator and guarantees a good airtightness. In addition, it avoids undesirable electromagnetic radiations from probes and makes possible the separate design of the transducer and its feeding circuit [6]. The pressure sensors based on these two planar technologies can be wirelessly detected and read from millimetre-wave Frequency-Modulated Continuous-Wave (FMCW) radars [7]. The three-dimensional radar imaging techniques allow actually the *in-situ* interrogation of such sensors, even in highly reflective electromagnetic environments [4, 5, 7-9].

This paper analyses the impact of standard bonding techniques on the performance of 23GHz pressure transducers: (1) the anodic bonding technique and (2)

* Corresponding author. maria-valeria.de-paolis@laas.fr
Tel: +33-5-61337878

the photoresist bonding approach. The anodic bonding process for assembling the membrane to the glass is the most promising solution because it allows the fabrication of airtight cavities without using additional materials between silicon and glass. However, as it may be performed in atmospheric pressure at lower temperature and it does not require high electrical field, the assembly using photoresist as an intermediate layer is easier to achieve than the one based on the anodic bonding. In addition, the electrical field used for the anodic bonding process may affect the electrical properties of glass or silicon, may cause mechanical constraints and produce eventual undesirable cracks in the silicon material.

We will show in this paper that, at the resonant frequency of the planar resonator, the measured transmission loss in probe-fed coplanar transducers is about 4dB when using photoresist bonding technique, while it is only of 2.55dB when applying the anodic bonding assembling technique. However, we show here for the first time that very high and unexpected transmission loss (>30dB) occurs when using anodic bonding technique to manufacture 23GHz aperture-coupled microstrip transducers. In order to understand why the anodic bonding process allows manufacturing low-loss probe-fed coplanar transducers but high-loss aperture coupled microstrip transducers, we carefully analyse the impact of such assembling technique on the performance of 23GHz pressure transducers.

2. Probe-fed coplanar transducers

The pressure transducer based on coplanar transmission lines is depicted in Fig. 1. It consists of a half-wavelength coupled-line resonator operating at 23GHz [3]. The glass material (Schott Borofloat B33 [10] with relative permittivity: 4.62 @ 26GHz, and loss tangent: 0.009 @ 26GHz) is selected as coplanar resonator substrate for its convenient physical and chemical properties (such as, thermal expansion behaviour, mechanical stability, etc.) for anodic bonding with silicon material. High resistivity silicon (HR-Si) substrate from BT electronics [11] is chosen for manufacturing the thin membrane.

Fig. 2 displays the simulated magnitude of the electric field (E-field) in the transducer of Fig. 1. The simulations are performed from the 3D full-wave software ANSYS HFSS. As expected, most of the E-field distribution at the resonant frequency is extended up to a depth of about 100-110µm from the planar resonator, while the higher E-field magnitudes are localized on the resonator surface (see [3] for details).

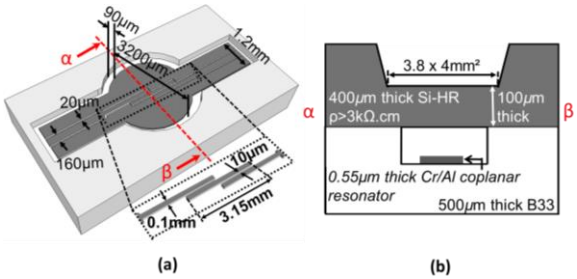

Fig. 1. Geometry of the pressure transducer consisting of a 23GHz coplanar resonator: (a) 3D view without the thin HR-Si membrane and (b) cross-sectional view with the membrane.

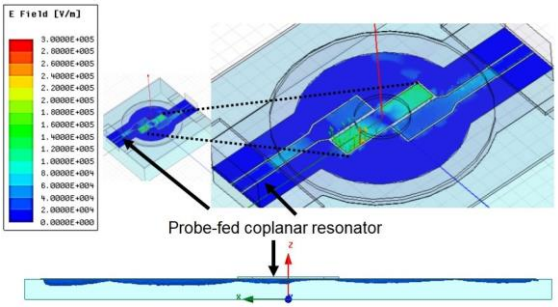

Fig. 2. Simulated (HFSS software) magnitude of the electric field in the 23GHz probe-fed coplanar pressure transducer shown in Fig. 1.

Two technological processes are considered for manufacturing the 23GHz probe-fed coplanar transducers, namely (i) the anodic bonding technique (see Fig. 3 in Section 2.1) and (ii) the photoresist bonding approach (see Fig. 5 in Section 2.2).

2.1. Anodic bonding assembling process

As illustrated in Fig. 3, after cleaning the 500µm thick glass substrate (step 1), the cavity is first patterned through the wet etching of glass using hydrofluoric acid (HF) for obtaining a deepness between 5µm and 15µm. This step requires the deposition and the patterning of a 150nm thick layer of chromium (Cr) and gold (Au) as hard mask (steps 2 and 3). These steps will define the diameter of the circular cavity (5500µm) and thus, the deflection of the membrane located above the planar resonator. The patterning of a 550nm thick chromium (Cr) and aluminium (Al) is performed for the planar resonator fabrication (steps 4 and 5). At the same time, the 400µm thick HR-Si substrate is processed. After cleaning (step 6), a 100nm thick layer of silicon nitride (Si_3N_4) is deposited (step 7). This layer is patterned and is used as a hard mask for the patterning of HR-Si substrate through TetraMethylAmmonium

Hydroxide (TMAH). The wet TMAH etching is performed at the back side (step 8) and the front side (step 9) in order to release the feed ports of the planar resonator, to etch the HR-Si substrate at the cavity level, and to get the 100µm thick membrane. Finally, the borosilicate glass substrate and HR-Si substrate are assembled using anodic bonding technique at 420°C and 600V in vacuum (step 10). Fig. 4 shows the manufactured transducer prototype.

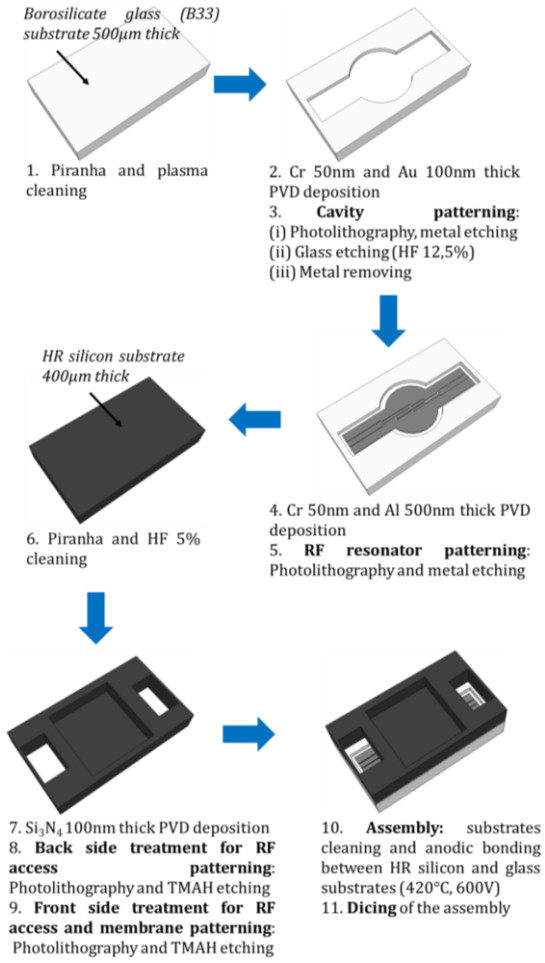

Fig. 3. Technological process for manufacturing the 23GHz probe-fed coplanar transducers using anodic bonding technique.

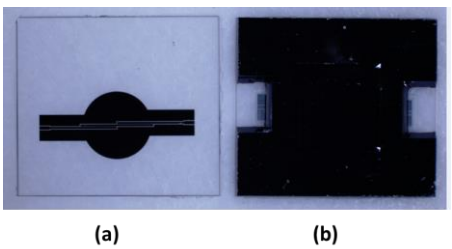

Fig. 4. Manufactured 23GHz probe-fed coplanar transducer (a) before and (b) after applying the anodic bonding technique.

2.2. Photoresist bonding technique

In this case, the bonding uses photoresist as an intermediate layer. It is performed between the glass substrate and the 100µm thick HR-Si chip obtained from substrate dicing. This assembling process is illustrated in Fig. 5. After the cleaning of the 500µm thick glass substrate (step 1), the planar resonator is manufactured from the patterning of the 550nm Cr/Al thick layer (steps 2 and 3). The photoresist provided by 3dis technologies [12] (relative permittivity: 3.5 @ 1MHz, and loss tangent: 0.02 @ 1MHz) is spincoated on the substrate to obtain a thickness between 5 and 15µm. Next, the layer is patterned to release the feed ports of the planar resonator and to form the 4000 µm x 3840 µm square cavity above the resonator (step 4). The assembling of the silicon die to the resonator on the glass substrate is performed by applying the thermo-compression at 110°C with the force of 110gram-forces (gF) during 5min (step 5).

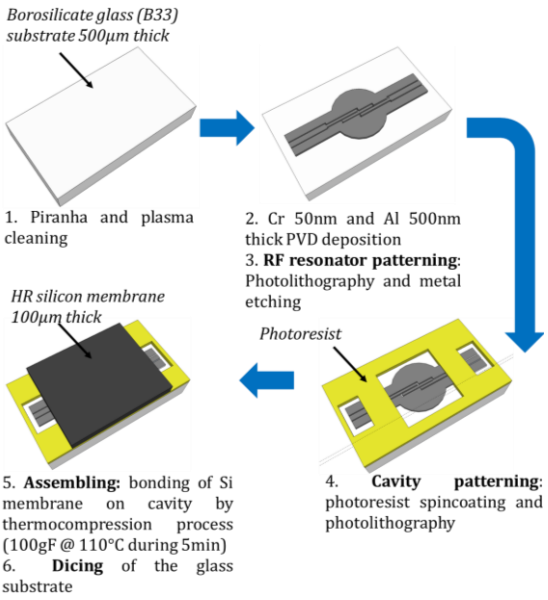

Fig. 5. Technological process for manufacturing the 23GHz aperture-coupled transducers using photoresist bonding technique.

2.3. Experimental results

For the two above-described manufacturing processes, the scattering parameters (S-parameters) are measured at the atmospheric pressure by using the PNA-X N5247A Network Analyzer and a manual probe station (Karl Süss PM8). Fig. 6 shows the experimental setup. In the insets c and d, the positions of the RF probes with respect to the two input ports of the coplanar resonator are indicated. The measurement accuracy is of ±0.05dB for the

S-parameters and ±13MHz for the frequency. Fig. 7 displays the measurement results obtained at the atmospheric pressure from the two manufacturing processes described in Sections 2.1 and 2.2.

For the photoresist bonding technique, the input reflection coefficient $|S_{11}|$ at the resonant frequency f_{res} is of -17.53dB, while the transmission loss $-|S_{21}|$ is of 4.09dB. When the anodic bonding assembling process is used (see Fig. 7), the measured $|S_{11}|$ is of -19.43dB and the transmission loss is of 2.55dB only.

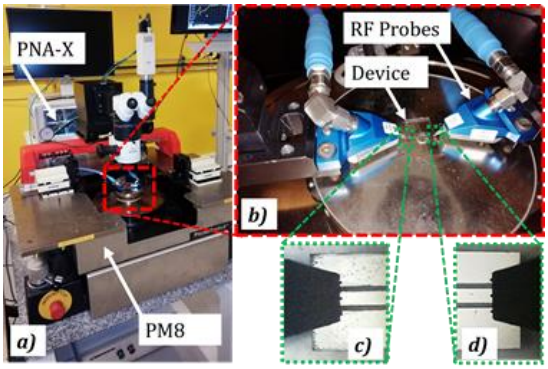

Fig. 6. Experimental setup used for measuring the S-parameters of the manufactured two-port probe-fed coplanar resonators.

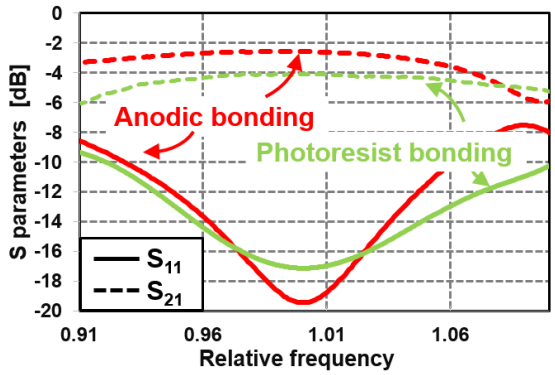

Fig. 7. Measured S-parameters at the atmospheric pressure as a function of the ratio f/f_{res} (where f_{res}=23GHz and f denotes the frequency) achieved for two assembling processes: photoresist bonding (in green) and anodic bonding (in red).

As our targeted application is the wireless interrogation of pressure sensors from a FMCW radar operating at 24GHz, the resonant frequency f_{res} lies in the radar operating bandwidth, and the transmission loss, sensor sensitivity, and full-scale range (or dynamic) over the applied pressure range are investigated in this bandwidth. Note that the sensor performance could be evaluated from the value of the input coefficient $|S_{11}|$ (see [4, 5] and [7] for details) or from the transmission losses in the radar operating bandwidth (see [8, 9] for details).

The experimental results achieved at the atmospheric pressure validate the technological steps of the two assembling processes described in Figs. 3 and 5 for manufacturing the 23GHz probe-fed coplanar transducers and demonstrate that the anodic bonding provides less transmission loss than the photoresist bonding.

3. Aperture-coupled microstrip transducers

The pressure transducer using microstrip transmission lines is depicted in Fig. 8.

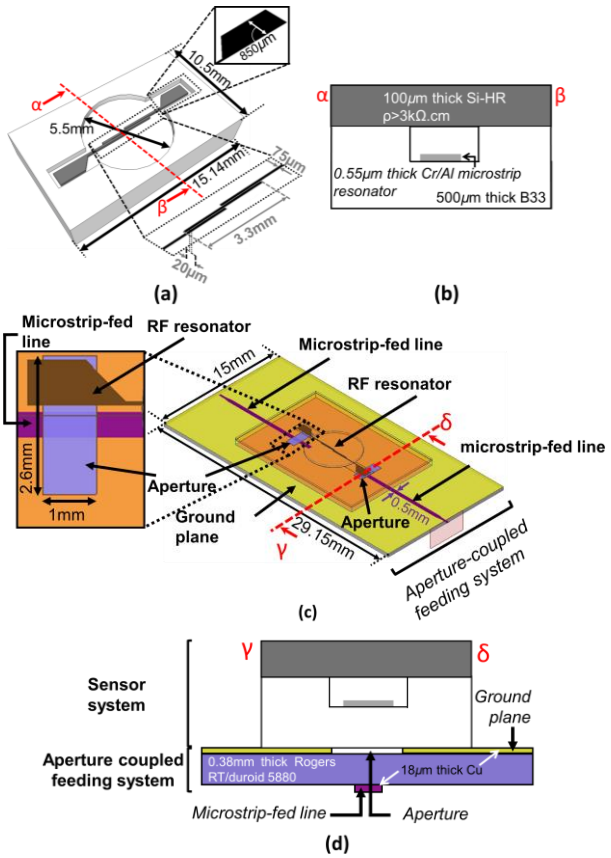

Fig. 8. Geometry of the 23GHz aperture-coupled pressure transducer: (a) 3D view of the sensor system without the thin silicon membrane, (b) cross-sectional view of the sensor system with the membrane, (c) 3D view without the membrane, and (d) cross-sectional view of the sensor system with its aperture-coupled feeding system.

It consists of the sensor and its aperture-coupled feeding systems. A half-wavelength parallel-edge coupled-line microstrip resonator operating at 23GHz was designed. The materials selected for the sensor substrate and the HR-Si membrane are the same as those used in Section 2, while a low-loss dielectric

substrate (Rogers RT/Duroid 5880 with relative permittivity: 2.2, and loss tangent: 0.0009 @10GHz, see [13] for details) is used for designing the aperture-coupled feeding system. The simulated magnitude of the E-field in the transducer is displayed in Fig. 9. Since the feeding system supplies electromagnetic power to the resonator through small apertures, the E-field distribution in the cross-section of the transducer is extended up to the whole glass thickness.

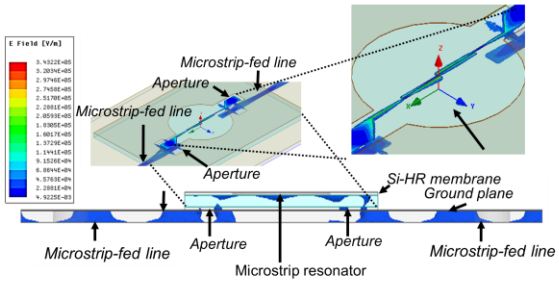

Fig. 9. Simulated (HFSS software) magnitude of the electric field in the 23GHz aperture-coupled microstrip pressure transducer shown in Fig. 8.

3.1. Two assembling processes

As detailed in Fig. 10, both the anodic bonding and photoresist bonding processes are investigated for manufacturing the 23GHz aperture-coupled microstrip transducers. A technological step is added for bonding the final transducer device to the aperture-coupled feeding system designed on the Rogers substrate (see Fig. 11) by using the epoxy glue as an intermediate layer. Fig. 12 shows the manufactured pressure transducer prototype.

3.2. Experimental results

At atmospheric pressure, the S-parameters are measured by means of the PNA-X N5247A Network Analyzer. As shown in Fig. 13, End Launch connectors (from Southwest Microwave) are used to connect to the two-port transducer to the network analyzer.

The measurement accuracies are identical to those given in Section 2.3. Fig. 14 displays the measured S-parameters of sensors obtained from the two manufacturing processes illustrated in Fig. 10 and Fig. 11. For the photoresist bonding, the input reflection coefficient $|S_{11}|$ at the resonant frequency is of -15.44dB, while the transmission loss $-|S_{21}|$ is of 5.40dB. This loss is then higher than the one provided by the probe-fed coplanar transducer (see Section 2.3). This was expected because the aperture–coupled feeding system brings more insertion loss than the direct probe-fed technique (see [6] for details).

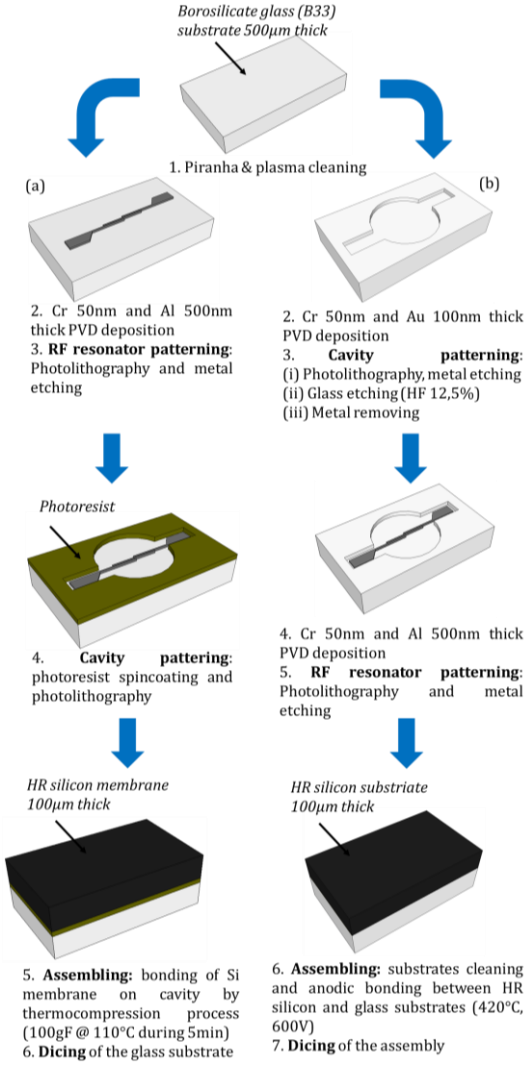

Fig. 10. Assembling processes for manufacturing the 23GHz aperture-coupled microstrip transducers: (a) photoresist bonding and (b) anodic bonding techniques.

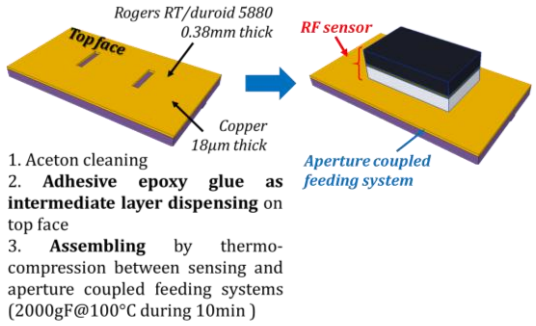

Fig. 11. Final assembling of the planar microstrip resonator and the aperture-coupled feeding systems.

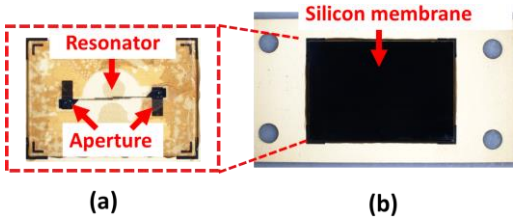

Fig. 12. Manufactured 23GHz pressure transducer using an aperture-coupled microstrip resonator. The photoresist bonding assembling process is chosen: (a) top view without the silicon membrane, and (b) top view with the silicon membrane.

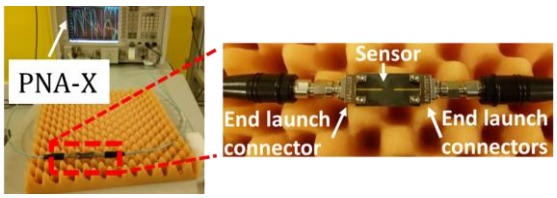

Fig. 13. Experimental setup used for measuring the S-parameters of the manufactured 23GHz microstrip two-port resonators.

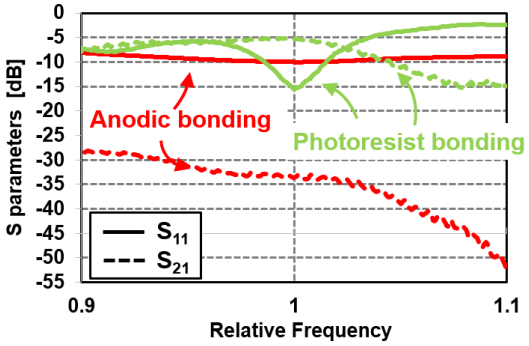

Fig. 14. Measured S-parameters at the atmospheric pressure as a function of the ratio f/f_{res} (where f_{res}=23GHz and f denotes the frequency) achieved for the sensors assembled from two manufacturing processes: photoresist bonding (in green) and anodic bonding (in red) assembling processes.

The S-parameters measurements were performed for seven sensors based on the photoresist bonding.

The relative shifts of resonant frequency with respect to the simulated resonant frequency f_{res0} (i.e., $(f_{res}-f_{res0})/f_{res}$[%], with f_{res0}=23GHz) were extracted for these seven pressure transducers and are depicted on the orange histogram of Fig. 15. The obtained averaged shift of relative resonant frequency with respect to the simulated resonant frequency is only of 1.5%. The blue histogram of Fig.15 shows the measured shifts of relative transmission losses with respect to the averaged measured transmission loss (i.e., $(-|S_{21}| - (-|S_{21mean}|))/ (-|S_{21}|)$[%], where $-|S_{21mean}|$ denotes the averaged measured transmission loss). In this case, the mean shift of the relative transmission

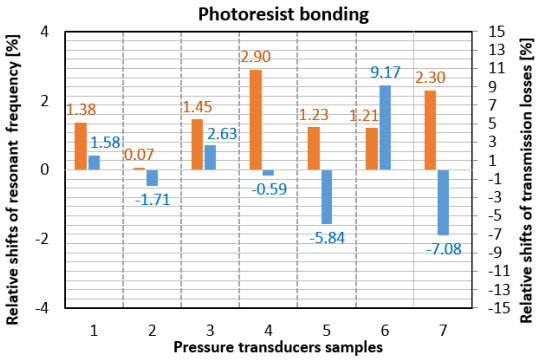

Fig. 15. Relative shifts of resonant frequency with respect to the simulated resonant frequency f_{res0} (orange histogram) (i.e., $(f_{res}-f_{res0})/f_{res}$[%], with f_{res0}=23GHz) and the measured relative shifts of transmission losses with respect to the averaged transmission loss (blue histogram) (i.e., $(-|S_{21}| - (-|S_{21mean}|))/ (-|S_{21}|)$[%], where $-|S_{21}mean|$ denotes the averaged measured transmission loss) achieved for the seven sensors assembled from photoresist bonding process.

losses is of -0.26%. Both results show the good reliability of the proposed technological process for manufacturing the devices.

The reproducibility of the measurement results was investigated for one sensor by measuring disconnecting and reconnecting it for ten times. The measured standard variation is respectively of 0.11GHz for the resonant frequency shift and of 0.33dB for the transmission losses.

For the anodic bonding technique, in the bandwidth $[f_{res}-0.1f_{res}, f_{res}+0.1f_{res}]$, the input reflection coefficient $|S_{11}|$ is greater than -10dB and a very high transmission loss (>30dB) is obtained. These values were unexpected and an intensive work is undergoing to find the origin of such high measured loss. Different sensor batches were manufactured and five sensors have been measured. Similarly, the measured transmission losses in the bandwidth of $[f_{res}-0.1f_{res}, f_{res}+0.1f_{res}]$ are very high, with a mean of 28dB.

Fig.16 illustrates the measured relative shifts of transmission losses with respect to the measured averaged transmission loss in these five pressure transducers. The mean shift of relative transmission losses is of -0.47%. While as for the input reflection coefficients $|S_{11}|$, they are always greater than -10dB.

In order to identify if the high transmission losses are due to an inadequate fabrication process, the impact of an eventual misalignment between the sensor and its feeding system was considered. The misalignments along the x- or the y-axes in the range of 0µm to 70µm were simulated by means of full-wave electromagnetic simulations.

The simulation results confirm that the

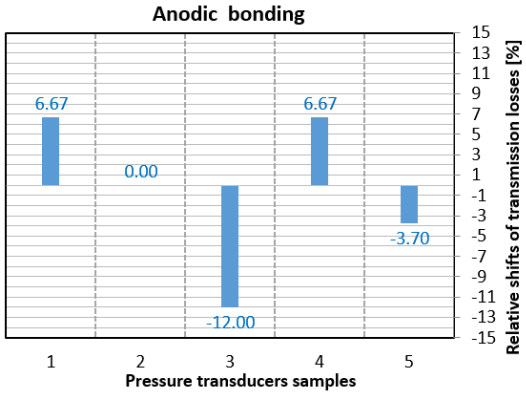

Fig. 16. Measured relative shifts of transmission losses (i.e., *(-|S21| – (-|S21mean|))/ (-|S21|)*[%], where -|*S21mean*| denotes the averaged measured transmission loss) achieved for the five sensors assembled from anodic bonding process.

transmission losses are not impacted by the misalignment, and the resonant frequency variation does not exceed 0.5% (see [6] for details).

Although the high transmission losses achieved by sensors based on anodic bonding technique is up-to-date unexplained, the experimental results obtained from photoresist bonding technique validate the technological steps described in Fig.s 10(a) and 11 for manufacturing the 23GHz aperture-coupled microstrip transducers.

4. Conclusion and future work

For the first time, the impact of anodic bonding technique on the transmission loss in pressure transducers is investigated in this paper.

The technological steps of photoresist and anodic assembling processes have been experimentally validated for manufacturing the 23GHz probe-fed coplanar transducers. Moreover, it was shown that anodic bonding provides less transmission loss in probe-fed coplanar transducers than the photoresist bonding.

The technological steps of the photoresist bonding process have been experimentally validated for manufacturing the 23GHz aperture-coupled microstrip transducers. However, very high transmission losses have been measured for different sensors when using the well-known anodic bonding process for manufacturing such transducers. Eventual misalignments between the sensor and its feeding system do not change significantly the transmission loss. We are performing further investigations for knowing if the unexpected high loss is due to the eventual modifications of the HR-Si membrane or/and the glass dielectric properties during the anodic bonding process. Because of different electric field distribution of the two transmission lines technologies, it is worth underlining that the possible variation of the glass properties does not invalidate the performance of probe-fed transducers fabricated from anodic bonding. Indeed, for the coplanar resonator, the E-field distribution occupies a region of 110µm depth in the glass, while for the microstrip resonator the distribution spreads throughout the glass thickness.

Acknowledgments

The authors wish to thank the Occitanie Region Council and European Fund for Regional Development for financial support through the CARANUC Project under Grant number [15053608] and EDF (Electricité de France) for funding part of this research work under Grant number [15057662]. This work was also partly supported by LAAS-CNRS micro and nanotechnologies platform members of the French RENATECH network.

References

[1] X. Zheng, W. Chen and X. Chen, “Stress in Si-glass anodic bonding and its effect on silicon piezoresistive pressure sensor,” *International Conference on Nano/Micro Engineered and Molecular Systems*, Xiamen, (2010), 524-527.

[2] T. Chen, L. Sun, M. Pan, Y. Wang, J. Liu and L. Chen, “Anodic bonding technology of slender glass tube and silicon in pressure sensor packaging,” *Electronics Packaging Technology Conference* (EPTC 2013), Singapore, (2013), 813-816.

[3] M. M. Jatlaoui, P. Pons, H. Aubert, “Pressure Micro-sensor based on Radio-Frequency Transducer,” *IEEE International Microwave Symposium*, Atlanta, Georgia, USA, pp. 1203-1206, 15-20 June 2008.

[4] J. Philippe, D. Henry, M. V. De Paolis, A. Rumeau, A. Coustou, S. Charlot, P. Pons, H. Aubert, “Wireless remote monitoring of packaged passive sensor for in-situ pressure measurement in highly reflective environments,” *2018 IEEE/MTT-S International Microwave Symposium - IMS*, Philadelphia, PA, 2018, pp. 47-50.

[5] Philippe J., De Paolis M.V., Henry D., Rumeau A., Coustou A., Pons P., Aubert H.,, “In-Situ Wireless Pressure Measurement Using Zero-Power Packaged Microwave Sensors”, *Sensors (Basel)*, 2019 Mar 13, 19(6).

[6] M. V. De Paolis, J. Philippe, A. Rumeau, A. Coustou, S. Charlot, H. Aubert, and P. Pons, “Aperture-coupled microstrip resonator for millimeter-wave passive pressure sensors,” Accepted for *TRANSDUCERS 2019*, 23-27 June 2019 - Berlin, Germany.

[7] D. Henry, P. Pons and H. Aubert, "3D scanning radar for the remote reading of passive electromagnetic sensors,"

2015 IEEE/MTT-S International Microwave Symposium, Phoenix, AZ, 2015, pp. 1-4.
[8] T. Marchal, J. Philippe, D. Henry, M. V. De Paolis, A. Coustou, P. Pons, H. Aubert, "Dual-Polarized Through-Wall Repeater for the Wireless Reading of Millimeter-wave Passive Sensors", Accepted for *APS/URSI 2019*, 7-12 July 2019 - Atlanta, Georgia, U.S.A.
[9] T. Marchal, J. Philippe, D. Henry, M. V. De Paolis, A. Coustou, P. Pons, H. Aubert, "Millimetre-Wave Interrogation of Passive Sensors Embedded Inside Closed Reverberant Environments from Dual-Polarized Passive Repeaters", Accepted for *EuMW 2019*, 29 September-4 October 2019, Paris, France.
[10] https://www.schott.com/borofloat/english/index.html
[11] https://bt-electronics.com/
[12] https://www.3dis-tech.com/
[13] http://www.rogerscorp.com/acs/products/32/rt-duroid-5880-laminates.aspx